Solar Cell Enhancement from Supercritical CO 2 Dye Surface Modification of Mesoporous TiO 2 Photoanodes

Maniam, Subashani; Skidmore, Melissa; Leeke, Gary A.; Collis, Gavin E.

DOI:
10.1002/cssc.202400560

Document Version
Publisher's PDF, also known as Version of record

Citation for published version (Harvard):
Maniam, S, Skidmore, M, Leeke, GA & Collis, GE 2024, 'Solar Cell Enhancement from Supercritical CO 2 Dye Surface Modification of Mesoporous TiO 2 Photoanodes', *ChemSusChem*.
https://doi.org/10.1002/cssc.202400560

ChemSusChem

Research Article
doi.org/10.1002/cssc.202400560

Chemistry Europe
European Chemical Societies Publishing

www.chemsuschem.org

Solar Cell Enhancement from Supercritical CO_2 Dye Surface Modification of Mesoporous TiO_2 Photoanodes

Subashani Maniam,*[a, b] Melissa Skidmore,[a] Gary A. Leeke,[c] and Gavin E. Collis*[a]

In recent years, in an effort to reach Net Zero Emissions, there has been growing interest by various academic and industry communities to develop chemicals and industrial processes that are circular, sustainable and green. We report the rapid, simple and effective surface modification of a porous metal oxide with organic dyes using supercritical carbon dioxide ($scCO_2$). Titanium dioxide (TiO_2) photoanodes were coated in very short times, under mild conditions and the excess dye recovered afterwards for reuse. The process obviates the need for conventional toxic solvents, the generation of unwanted waste streams, and more importantly, we see an unexpected device performance enhancement of 212 and 163% for TerCOOTMS, **2a** and TerCN/COOTBDMS, **4** dyes, respectively, when compared to the conventional solvent deposition method.

Introduction

As countries transition towards Net Zero Emissions, there are significant efforts to address the life cycle of technologies, from the types of chemicals that are used (critical *vs* sustainable), the way they are processed and manufactured into products and end-of-life (EoL) management, from the 3Rs (reduce, reuse and recycle) and waste minimization, whilst considering the energy required and emissions produced. An area well suited for improvement is the chemicals industry, where shifting towards sustainable chemical feedstocks, environmentally friendly chemicals[1] and chemical processes using green methods, and addressing waste streams (linear *vs* circular) and obtaining value from waste are all viable options.[1b,2]

The decoration of inorganic particles and thin films with organic materials (inorganic-organic hybrid systems) continues to attract interest in areas ranging from energy generation and storage, organic electronics,[3] composite materials,[4] self-assembled monolayers (SAMs),[5] nanoparticle diagnostics for biological and environmental systems, and drug-delivery applications.[4c,6] The grafting of materials onto a surface of a substrate imparts changes to the chemical, optical, electronic and physical properties of the hybrid material; understanding what is occurring at the inorganic-organic interface[7] is not trivial because of the domain scale, complex multi-layered systems and non-homogeneous boundary layers. In energy transfer systems, non-uniform coverage of the surface with a dye typically manifests in poor device efficiency and long-term stability. This can be ascribed to surface defects, and unfavourable charge recombination and electrochemical processes leading to unwanted chemical reactions located at the inorganic-organic interface. This is a key challenge to address in many current and emerging renewable energy generation and storage, and sensor technologies.

Here, we investigated using $scCO_2$ as a green solvent to deposit simple dyes onto photoanodes and evaluate their performance in dye-sensitized solar cells (DSSCs). This photoelectrochemical cell consists of a mesoporous metal oxide photoanode decorated with a layer of light-harvesting dye and a redox electrolyte sandwiched between two electrodes.[8] Mesoporous TiO_2 is the material of choice due to its robust physical properties, high electron mobility and the accessibility of different particle sizes to assist in scattering light within the photoanode to maximize light uptake by the dye.[9] Whilst significant effort continues to focus on the design and development of new dyes,[10] incomplete dye coverage and poor attachment to the metal oxide surface[11] can result in unwanted electrochemical reactions from the redox electrolyte and dye desorption;[9c,12] both these factors impact the maximum cell efficiency attainable and long-term device durability. $scCO_2$ has received renewed interest over the last decade as a green solvent for deposition of materials onto specific substrates,[13] controlling particle size during synthesis,[14] solvent annealing[15] and chemical processing[16] of materials at surfaces[13a,17] across a variety of different applications.

[a] *Dr. S. Maniam, Dr. M. Skidmore, Dr. G. E. Collis*
Manufacturing, Advanced Materials and Processes, CSIRO
Clayton South, Victoria, 3168, Australia
E-mail: subashani.maniam@rmit.edu.au
Gavin.Collis@csiro.au

[b] *Dr. S. Maniam*
School of Science, STEM College, RMIT University
Melbourne, Victoria, 3001, Australia
E-mail: Subashani.Maniam@rmit.edu.au

[c] *Prof. Dr. G. A. Leeke*
School of Chemical Engineering, University of Birmingham,
Birmingham, B15 2TT, UK

Supporting information for this article is available on the WWW under https://doi.org/10.1002/cssc.202400560

Results and Discussion

Protecting Group Strategy

Previous studies using $scCO_2$ with high molecular weight dyes required co-solvents[18] or custom perfluoroalkyl-dye to be synthesized to increase the solubility of the dye.[12c,19] Recently, studies around the EoL of fluorinated chemicals from a broad range of applications,[20] including emerging lithium-ion batteries technologies,[21] has raised worrying concerns around the presence of per- and polyfluoroalkyl substances (PFAS)[22] that may pose environmental issues[1a] if not managed or disposed of properly:[23] there has been a call to ban fluorinated chemicals and fines imposed.[21,24] Thus in some applications if green processing technologies or safer chemicals could be employed it could offer significant advantages compared to currently organic solvents and hazardous chemicals used in manufacturing, which produces unwanted hazardous waste and are energy and time intensive.

Very simple organic dyes TerCOOH **1** and TerCN/COOH **3** where chosen as both the carboxylic acid and cyanoacrylic acid binding groups are commonly used to anchor the dye to the metal oxide surface in magnetic and energy transfer applications.[6a,25] To solubilize these dyes for use in $scCO_2$ a number of silyl-masked ester derivatives **2a-c** and **4** were synthesized. Using standard protecting group chemistry, target terthiophene carboxylic ester derivatives, TerCOOTMS **2a**, TerCOOTBDMS **2b** and TerCOOTIPS **2c**, were prepared in excellent yields (>92%) from the corresponding terthiophene carboxylic acid **1** (Scheme 1). However, attempts to transform terthiophene cyanoacrylic acid **3** into the analogous family of terthiophene cyanoacrylic acid silyl-ester derivatives proved significantly difficult. Attempts to synthesize and isolate the trimethylsilyl or triisopropyl ester derivatives of TerCN/COOH **3** were undertaken, however, we found the products to be extremely unstable. We attributed the poor stability to the strong electron withdrawing nature of the adjacent cyano-group favouring rapid cleavage of the silyl group. Instead, the bulky *tert*-butyldimethylsilyl ester derivative, TerCN/COOTBDMS **4** was successfully synthesized and isolated (Scheme 1 and SI for full experimental details).

Spectroscopic and Electrochemical Performance, and $scCO_2$ Solubility

The spectroscopic and electrochemical properties of both benchmark dyes **1** and **3** were studied and compared. The UV-Vis absorption spectra of TerCOOH **1** and TerCN/COOH **3** were evaluated in dichloromethane (DCM) (Figure 1) and showed an absorption maximum at 372 nm ($\varepsilon = 22\,852\ M^{-1}cm^{-1}$) and 446 nm ($\varepsilon = 26\,542\ M^{-1}cm^{-1}$), respectively. While the molar absorption coefficient of **3** is slightly higher, the presence of the cyano-acrylic linker results in a bathochromic shift in the absorption spectrum when compared to **1**. To understand the electronic properties of TerCOOH **1** and TerCN/COOH **3**, cyclic voltammograms (CV) were recorded in dimethylformamide (DMF). The first oxidation and reduction potentials were used to determine the HOMO and LUMO levels of the compounds. The LUMO levels of TerCOOH **1** (−3.54 eV) and TerCN/COOH **3** (−2.76 eV) are more positive than the potential of TiO_2 conduction band (−3.90 eV) allowing electron injection from the dye upon excitation.[26] TerCOOH **1** and TerCN/COOH **3** have HOMO levels of −5.67 eV and −5.56 eV, respectively, that are more positive than the I^-/I_3^- redox couple (−4.85 V)[8c,10,26–27] thus providing the driving force for dye regeneration. The studies indicate that changes in the absorption wavelength and the LUMO energy levels in both compounds are caused by the different binding groups employed; thus TerCOOH **1** and TerCN/COOH **3** should both provide a suitable photo-response for the aim of the current study (see SI, Table S1).

Previously in organic electronics research and materials discovery areas[12c,28] we have successfully employed computational aided modelling to select, design and synthesize new compounds that has enabled better selection of suitable candidates. DFT calculation of TerCOOH **1** and TerCN/COOH **3** (Table 1) show extremely good alignment and trend well with experimental data collected and could be used in future to refine the properties of these dyes as required for specific end-use applications.

The family of terthiophene acid **1** derivatives with different silyl groups showed high solubility in $scCO_2$, whilst the free acid was marginally soluble. The solubility of silyl protected dyes **2a**, **2b** and **2c** was greatly improved (459–487 mg/kg in $scCO_2$) with the solubility increasing with the size of the silyl group (i.e.

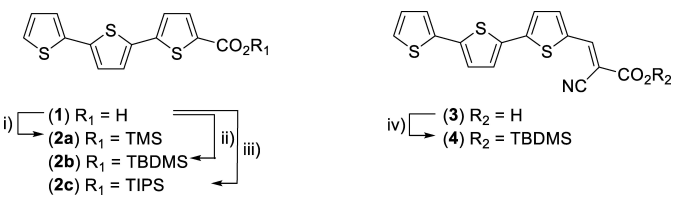

Scheme 1. Chemical structure of TerCOOH **1** and synthesis of TerCOO-silyl derivatives **2a–2c**.[a] Chemical structure of TerCN/COOH **3** and synthesis of TerCN/COOTBDMS **4**.[b] [a] Reagents and conditions: (i) 1,3-bis(trimethylsilyl)-urea, anhydrous CH_2Cl_2, reflux, 2 hours, yield 92%; (ii) chloro-*tert*-butyldimethylsilane, imidazole, anhydrous CH_2Cl_2, RT, 16 hours, yield 93% (iii) chloro-trisisopropylsilane, imidazole, anhydrous CH_2Cl_2, RT, 16 hours, yield 98%. [b] Reagents and conditions: (iv) chloro-*tert*-butyldimethylsilane, imidazole, anhydrous CH_2Cl_2, RT, 16 hours, 94%.

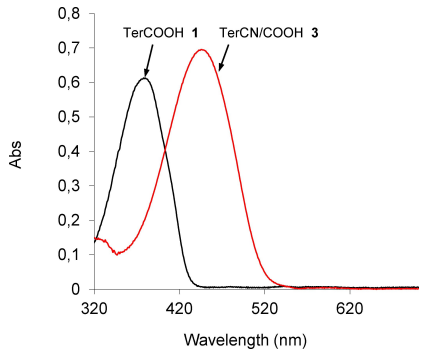

Figure 1. UV-Visible absorption spectra of TerCOOH **1** and TerCN/COOH **3** in DCM.

Table 1. Calculated HOMO and LUMO Levels of TerCOOH **1** and TerCN/COOH **3**.

Head 1[b]	TerCOOH **1**	TerCN/COOH **3**
3D HOMO orbitals	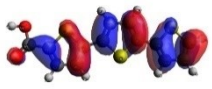	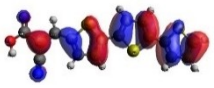
3D LUMO orbitals	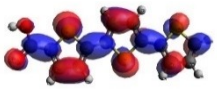	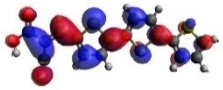
HOMO (Haartree)	−0.21264	−0.22131
LUMO (Haartree)	−0.09445	−0.12427
E_{HOMO} (eV)	−5.79	−6.02
E_{LUMO} (eV)	−2.57	−3.38

TIPS > TBDMS > TMS > H) (Table 2). The trend for the solubility is also consistent with the stability of the silyl-ester group with the bulky TIPS being the most stable amongst the silyl protecting groups used in this study.

Table 2. Solubility data for terthiophene dyes measured in $scCO_2$ at 14 MPa and 50 °C.

Entry	Dye	Solubility in $scCO_2$ (mg/kg)
1	TerCOOH **1**	0.5
2	TerCOOTMS **2a**	459
3	TerCOOTBDMS **2b**	470
4	TerCOOTIPS **2c**	487
5	TerCN/COOH **3**	0[a]
6	TerCN/COOTBDMS **4**	5.5

[a] No recorded solubility.

In relation to silyl ester stability data it is also well established that the larger the silyl group the slower the rate of cleavage of the Si–O bond.[29] Interestingly, the introduction of the extremely polar acrylic functionality and using the TBDMS protecting group, had less impact to the overall solubility of the dye: the TerCN/COOH **3** being completely insoluble in $scCO_2$ and the silyl derivative being marginally better (5.5 mg/kg).

Photovoltaic Performance

Analysis of the photovoltaic performance of these dyes deposited by conventional organic and $scCO_2$ solvent (see SI, Figure S7) is presented in Table 3 (and see SI, Table S2). The free terthiophenecarboxylic acids, dyes **1** and **3** were deposited onto metal oxide surfaces using organic solvent methods reported previously.[6a,25a,c,d,g,26,30] While ethanol (EtOH) and DCM are commonly used, we found that TerCOOH **1** had very poor solubility in EtOH and DCM gave a moderate energy conversion efficiency (ECE) value (Entry 2). Instead, the best ECE value for TerCOOH **1** was achieved using a new binary solvent system of ethanol with acetonitrile (MeCN) (Entry 2), while efforts using just $scCO_2$ produced negligible ECE response as expected. Irrespective of the silyl protecting group used (i.e., **2a**, **2b** and **2c**), the dye deposition time was dramatically reduced from 15–24 to 2 hrs and the ECE values increased up to ~200 to 300% (Entries 3, 4, 5 and 6). A clear trend was also observed between the size and stability of the silyl-protecting group, solubility and ECE performance. Although solubility is an important parameter, smaller more labile groups gave higher ECE values under these conditions, where the TMS protecting group of **2a** provides an excellent compromise of solubility and reactivity towards the metal oxide surface. This assumption is supported by experiments where variation of time for exposure **2b** to the TiO_2 surface that produced a slight increase in ECE from 1.21 to 1.42%, suggesting further room for optimizing the ECE performance by variation of time and pressure parameters. To under-

Table 3. Photovoltaic cell performance of TerCOOR and TerCN/COOR dyes deposited from conventional organic solvents (0.3 mM, 15 hrs) and $scCO_2$ (14 MPa, 50 °C, 2 hrs), respectively.

Entry and dye	Solvent[a]	J_{sc} (mA/cm^2)	V_{oc} (mV)	FF	ECE (%)
1. TerCOOH **1**	DCM	2.24	468	0.54	0.57 ± 0.03
2. TerCOOH **1**	EtOH/MeCN	2.77	488	0.52	0.70 ± 0.04
3. TerCOOH **1**	$scCO_2$	0.57	470	0.60	0.17 ± 0.02
4. TerCOOTMS **2a**	$scCO_2$	5.77	470	0.58	1.80 ± 0.02
5. TerCOOTBDMS **2b**	$scCO_2$	3.64	510	0.65	1.21 ± 0.01
6. TerCOOTIPS **2c**	$scCO_2$	3.73	506	0.60	1.12 ± 0.01
7. TerCOOTBDMS **2b***	$scCO_2$	4.77	560	0.53	1.42 ± 0.02
8. TerCN/COOH **3**	EtOH/MeCN	5.52	510	0.50	1.43 ± 0.01
9. TerCN/COOH **3**	DCM	4.50	567	0.67	1.68 ± 0.05
10. TerCN/COOTBDMS **4**	$scCO_2$	7.76	590	0.60	2.74 ± 0.03

[a] DCM – dichloromethane, EtOH – ethanol, MeCN – acetonitrile.

stand the origins of the improved performance we examined the current-voltage (*I-V*) and incident photon to current efficiency (IPCE) curves for TerCOOH **1** deposited by conventional DCM and $scCO_2$ (Figure 2). In both these plots there is an increase in current and voltage and light absorption properties of the photoanode when the terthiophene dye is deposited using $scCO_2$, which is impressive given the short contact times (2 *vs* 15–24 hrs). Examination of the terthiophene acrylic dye also reveals a similar trend when using $scCO_2$ and the problems associated with identifying and determining the best solvent system to use when using the conventional organic solvent method.[11]

In contrast, although ECE values for TerCOOH **1** were higher using EtOH/DCM solvent mix, the opposite was observed for TerCN/COOH **3** where DCM was better. Our results for dye **3** were significantly higher than reported ECEs of 0.60% **15** and 0.69% **16** when deposited from MeCN/*t*-butyl alcohol (1:1) and methanol over a 20 hr period, respectively. Under our conditions, both MeCN/EtOH (1:1 v/v) (Table 3, Entry 8) and DCM (Table 3, Entry 9) gave ECE values with an excess of 180% improvement in cell performance compared to literature reports. The improvement could be attributed to several factors, including the different dye soaking solvent and time, electrolyte system and source of the TiO_2 photoanode used. TerCN/COOH **3** showed extremely low solubility in $scCO_2$ (Table 2, Entry 5) owing to the polar cyano-acrylic acid binding group and not surprisingly no photo-response was observed. However, the masked silyl derivative TerCN/COOTBDMS **4**, even with limited solubility in $scCO_2$ (5.5 mg/kg), was deposited from $scCO_2$ in 2 hrs and produced a dramatic 63% increase in J_{sc} and V_{oc} affording an ECE value of 2.74%. This is reflected in the *I-V* and IPCE graphs for conventional and $scCO_2$ deposited dye device data shown (see SI, Figure S8). Overall increases in J_{sc}, V_{oc} and better light to current conversion than TerCN/COOH **3** were observed when compared to the dye deposited by conventional solvents. Most importantly, the IPCE peak shape has not changed, however the intensity has increased which we propose can be attributed to greater dye loading onto the photoanode.

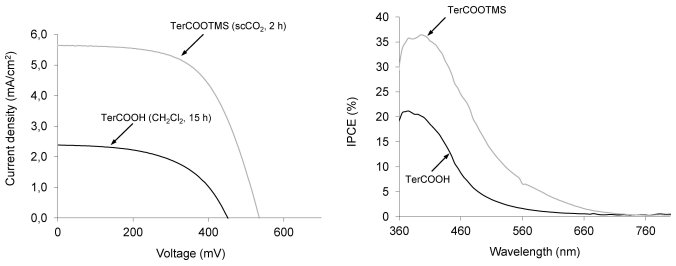

Figure 2. Current-voltage curves measured under simulated AM 1.5 sunlight at 100 mW/cm^2 for TerCOOH **1** (conventional dye soaking: 0.3 mM in EtOH: DCM, 15 hrs) and from TerCOOTMS **2a** ($scCO_2$, 14 MPa, 50 °C, 2 hrs).

Dye Loading and Desorption

To confirm the different dye loading between the organic solvent and $scCO_2$ methods, dye desorption studies were performed. TerCOOH **1** and TerCN/COOH **3** and their silyl derivatives, TerCOOTMS **2a** and TerCOOTBDMS **2b**, and TerCN/COOTBDMS **4** were subjected to dye deposition using conventional (see SI, Table S3, Entries 1 and 4) and $scCO_2$ (see SI, Table S3, Entries 2, 3 and 5) methods, respectively. Darker dye colouration of TiO_2 photoanodes was obtained with the $scCO_2$ method than conventional solvents. Dye photoanode loading was determined by desorption studies using basic ethanolic solution (see SI, Table S4).[30a,31] Higher dye loadings were obtained using $scCO_2$, TerCOOTMS **2a** and TerCOOTBDMS **2b** compared to the conventional method, TerCOOH **1** (see SI, Table S4, Entries 2 and 3 vs 1). With TerCN/COOH **3**, complete dye desorption was obtained from the photoanodes of the conventional method (see SI, Table S4, Entry 4). Surprisingly, photoanodes from $scCO_2$ deposition method using TerCN/COOTBDMS **4** still showed colouration after the desorption process indicative of the presence of dye (see SI, Table S4, Entry 5): the origins of this difference between conventional and $scCO_2$ deposition for this binding group is unclear[12d] but could be due to different packing densities and binding modes using different solvent and pressures.[25b,32]

To determine where the silyl protecting group was migrating during the deposition process FTIR-ATR and ^{1}H NMR spectroscopy studies were undertaken.[6f,13c, 33] Both dyes, TerCOOH **1** and TerCN/COOH **3**, deposited using conventional solvents showed different peaks in their FTIR-ATR spectra. TerCOOH **1** gave a weak signal at 1616 cm^{-1} which was assigned to the stretching vibrations of the C=O bond (see SI, Figure S9). When the TerCOOTMS **2a** dye precursor was used in $scCO_2$ to deposit it on the TiO_2 photoanode we observed a nearly identical IR spectrum when compared with conventional organic solvent dye soaking conditions. The lack of any silicon residue suggests that upon attachment of the dye on the photoanode, the silicon by-product most likely formed is the trimethylsilanol (TMS-OH) and/or hexamethyldisiloxane (TMS-O-TMS), respectively. TMS-OH and TMS-O-TMS both have relatively low boiling points (b.p. 99 and 100–101 °C, respectively) and could be released upon depressurization of the $scCO_2$ vessel, which this is supported by ^{1}H NMR spectroscopy analysis of the vented CO_2 gas showing silicon signals (see SI, Figure S11). In contrast, when TerCOOTBDMS **2b** was used we observed some new signals at 1051 cm^{-1} and 1155 cm^{-1} in the FTIR spectrum that we attributed to the formation Si–O–Ti bonds (see SI, Figure S9).[13c,33a,e,f,34] We propose that this bulky protecting group also forms analogous silicon by-products, TBDMS-OH and TBDMS-O-TBDMS. These silicon materials have higher boiling points compared to TMS-materials of 139 °C/739 mmHg and 191–193 °C/760 mmHg, respectively. Based on the boiling point and presence of the Si–O signals in the IR, this suggests that the TBDMS-OH by-product is less likely to be removed upon depressurization and can react with the TiO_2 surface. With TerCN/COOH **3** two strong signals at 1597 cm^{-1} and 1392 cm^{-1} were observed and attributed to the asymmetric and symmetric

mode of carboxylate group, respectively (see SI, Figure S10).[33f] As with TerCOOTBDMS **2b**, TerCN/COOTBDMS **4** showed similarities with a peak at 1051 cm^{-1} corresponding to the Si–O–Ti stretching,[34] while peaks at 1157 cm^{-1} and 1211 cm^{-1}, and sharp bands between 1220–1250 cm^{-1} can be assigned to the Si–C stretching indicative of silyl groups attached to the photoanode.

Based on previous efforts of post-silane modify dye coated photoanodes[34–35] and the current work of *in situ* dye/silane deposition, the presence of silanes do not seem to be detrimental to the photovoltaic performance (Figure 3). This difference between the TerCN/COOTBDMS **4** desorption studies by using conventional and $scCO_2$ methods, where there was a colouration difference after ethanolic treatment, presumably is related to the *in situ* silyl/dye deposition process occurring only in $scCO_2$, altering the surface properties (Figure 3).

Conclusions

In summary, with processes that are circular, sustainable and green in mind, we have demonstrated that small oligothiophene dyes with masked silyl-binding group can be deposited in $scCO_2$ to produce significant increase in photovoltaic performance. Both TerCOOH **1** and TerCN/COOH **3** were evaluated in DSSC devices, where dyes were deposited by conventional and their silyl derivatives using $scCO_2$ methods. In conventional organic solvents, TerCOOH **1** and TerCN/COOH **3** produced ECE of 0.60% and 1.68%, respectively. However, dramatic increases in photovoltaic response were obtained when the dyes were deposited using $scCO_2$ with their binding groups masked as labile silyl esters, TerCOOTMS **2a** (ECE 1.80%) and TerCN/COOTBDMS **4** (ECE 2.74%). Additionally, the dye deposition time has been significantly reduced from 15–24 hours in conventional soaking solvent to 2 hours using $scCO_2$ method and easily recovered after depressurization. Established and new dyes for simple surface modification could easily be adapted to this $scCO_2$ deposition protocol and this approach could be useful in the controlled chemical decoration of metal particles using a green solvent for a number of different end-use applications.

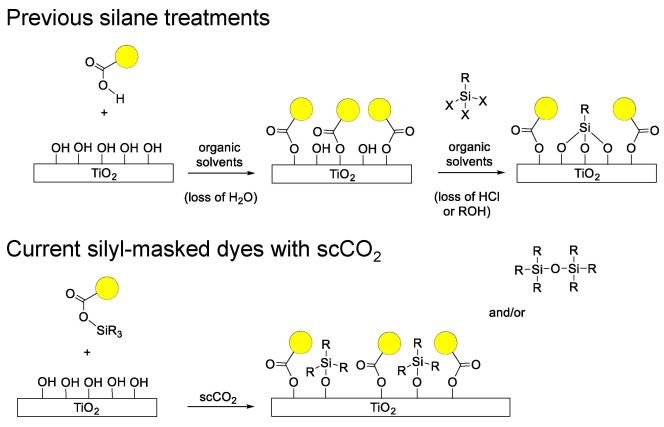

Figure 3. Schematic showing a comparison of the two different methods of silane surface treatments via; a) conventional organic solvent dye coated photoanode and b) $scCO_2$ silyl-masked dye methods.

Acknowledgements

We thank CSIRO Manufacturing for support and award of a postdoctoral fellowship to SM. We thank Professor Andrew Holmes for his fruitful discussions and suggestions on this topic. We also thank Tiejun Lu for undertaking the solubility measurements in $scCO_2$. Open Access publishing facilitated by RMIT University, as part of the Wiley - RMIT University agreement via the Council of Australian University Librarians.

Conflict of Interests

No conflicts to declare.

Data Availability Statement

The data that support the findings of this study are available from the corresponding author upon reasonable request.

Keywords: supercritical carbon dioxide · green solvent · solar cell · terthiophene · dye deposition

[1] a) T. Ruan, P. Li, H. Wang, T. Li, G. Jiang, *Chem. Rev.* **2023**, *123*, 10584–10640; b) M. Yang, L. Chen, J. Wang, G. Msigwa, A. I. Osman, S. Fawzy, D. W. Rooney, P.-S. Yap, *Environ. Chem. Lett.* **2022**, *21*, 55–80.
[2] a) S. Gressler, F. Part, S. Scherhaufer, G. Obersteiner, M. Huber-Humer, *Sustain. Mater. Techn.* **2022**, *34*; b) A. Cannon, S. Edwards, M. Jacobs, J. W. Moir, M. A. Roy, J. A. Tickner, *RSC Sustainability* **2023**, *1*, 2092–2106.
[3] Y. Wen, Y. Liu, Y. Guo, G. Yu, W. Hu, *Chem. Rev.* **2011**, *111*, 3358–3406.
[4] a) Q. Zhang, M. Li, L. Li, D. Geng, W. Chen, W. Hu, *Chem. Soc. Rev.* **2024**; b) A. Kumar, D. W. Chang, J.-B. Baek, *Energy Fuels* **2023**, *37*, 17782–17802; c) M. Prajapati, V. Singh, M. V. Jacob, C. Ravi Kant, *Renewable Sustainable Energy Rev.* **2023**, *183*.
[5] J. J. Gooding, F. Mearns, W. Yang, J. Liu, *Electroanalysis* **2003**, *15*, 81–96.
[6] a) W. J. E. Beek, R. A. J. Janssen, *J. Mater. Chem.* **2004**, *14*, 2795–2800; b) X. Duan, P. Wang, L. He, Z. He, S. Wang, F. Yang, C. Gao, W. Ren, J. Lin, T. Chen, C. Xu, J. Li, A. Wu, *Adv. Mater.* **2024**, e2311548; c) N. Zhao, Z. Jiao, L. Chen, Z. Liu, X. Zhao, F.-J. Xu, *Accounts Mater. Res.* **2023**, *4*, 1068–1082; d) C. C. Fleischer, C. K. Payne, *Acc. Chem. Res.* **2014**, *47*, 2651–2659; e) H. Wu, S. Zhang, J. Zhang, G. Liu, J. Shi, L. Zhang, X. Cui, M. Ruan, Q. He, W. Bu, *Adv. Funct. Mater.* **2011**, *21*, 1850–1862; f) A. M. López-Periago, W. Sandoval, C. Domingo, *Appl. Surf. Sci.* **2014**, *296*, 114–123; g) B. Bhartia, S. Das, S. Jayaraman, M. Sharma, Y. P. Ting, C. Troadec, S. P. Madapusi, S. R. Puniredd, *Langmuir* **2023**, *39*, 9564–9578.
[7] H. Ma, H. L. Yip, F. Huang, A. K. Y. Jen, *Adv. Funct. Mater.* **2010**, *20*, 1371–1388.
[8] a) M. A. M. Al-Alwani, A. B. Mohamad, N. A. Ludin, A. A. H. Kadhum, K. Sopian, *Renewable Sustainable Energy Rev.* **2016**, *65*, 183–213; b) M. Wei, Y. Konishi, H. Zhou, M. Yanagida, H. Sugihara, H. Arakawa, *J. Mater. Chem.* **2006**, *16*; c) J. Gong, K. Sumathya, Q. Qiao, Z. Zhoub, *Renewable Sustainable Energy Rev.* **2017**, *68*, 234–246.
[9] a) D. Sengupta, P. Das, B. Mondal, K. Mukherjee, *Renewable Sustainable Energy Rev.* **2016**, *60*, 356–376; b) J. Ferber, J. Luther, *Sol. Energy Mater. Sol. Cells* **1998**, *54*, 265–275; c) S. Tatay, S. A. Haque, B. O'Regan, J. R. Durrant, W. J. H. Verhees, J. M. Kroon, A. Vidal-Ferran, P. Gaviña, E. Palomares, *J. Mater. Chem.* **2007**, *17*, 3037–3044; d) H.-J. Koo, J. Park, B. Yoo, K. Yoo, K. Kim, N.-G. Park, *Inorg. Chim. Acta* **2008**, *361*, 677–683.
[10] A. Sen, M. H. Putra, A. K. Biswas, A. K. Behera, A. Groβ, *Dyes Pigm.* **2023**, *213*.

[11] H. Tian, X. Yang, R. Chen, R. Zhang, A. Hagfeldt, L. Sun, *J. Phys. Chem. C* **2008**, *112*, 11023–11033.
[12] a) P. Wen, M. Xue, Y. Ishikawa, H. Itoh, Q. Feng, *ACS Appl. Mater. Interfaces* **2012**, *4*, 1928–1934; b) C. Chen, X. Yang, M. Cheng, F. Zhang, L. Sun, *ChemSusChem* **2013**, *6*, 1270–1275; c) S. Maniam, A. B. Holmes, G. A. Leeke, A. Bilic, G. E. Collis, *Org. Lett.* **2015**, *17*, 4022–4025; d) K. C. Liao, H. Anwar, I. G. Hill, G. K. Vertelov, J. Schwartz, *ACS Appl. Mater. Interfaces* **2012**, *4*, 6735–6746; e) C.-J. Liang, C. P. Kumar, C.-T. Li, J. T. Lin, *Asian J. Org. Chem.* **2018**, *7*, 819–828; f) B. A. Gregg, F. Pichot, S. Ferrere, C. L. Fields, *J. Phys. Chem. B* **2001**, *105*, 1422–1429; g) Q. Wang, S. Ito, M. Gratzel, F. Fabregat-Santiago, I. Mora-Sero', J. Bisquert, T. Bessho, H. Imai, *J. Phys. Chem. B* **2006**, *110*, 25210–25221.
[13] a) A. J. Hunt, V. L. Budarin, J. W. Comerford, H. L. Parker, V. K. Lazarov, S. W. Breeden, D. J. Macquarrie, J. H. Clark, *Mater. Lett.* **2014**, *116*, 408–411; b) Y. Nakayasu, S. Sokabe, Y. Hiraga, M. Watanabe, *Chem. Commun.* **2023**, *59*, 3079–3082; c) R. D. Weinstein, D. Yan, G. K. Jennings, *Ind. Eng. Chem. Res.* **2001**, *40*, 2046–2053.
[14] N. Esfandiari, *J. Supercrit. Fluids* **2015**, *100*, 129–141.
[15] B. X. Dong, J. A. Amonoo, G. E. Purdum, Y. L. Loo, P. F. Green, *ACS Appl. Mater. Interfaces* **2016**, *8*, 31144–31153.
[16] a) K. Taniguchi, E. N. Kusumawati, H. Nanao, C. V. Rode, O. Sato, A. Yamaguchi, M. Shirai, *New J. Chem.* **2023**, *47*, 12561–12569; b) C. Boyère, C. Jérôme, A. Debuigne, *Eur. Polym. J.* **2014**, *61*, 45–63; c) T.-R. Kuang, H.-Y. Mi, D.-J. Fu, X. Jing, B.-y. Chen, W.-J. Mou, X.-F. Peng, *Ind. Eng. Chem. Res.* **2015**, *54*, 758–768.
[17] a) B. Bhartia, N. Bacher, S. Jayaraman, S. Khatib, J. Song, S. Guo, C. Troadec, S. R. Puniredd, M. P. Srinivasan, H. Haick, *ACS Appl. Mater. Interfaces* **2015**, *7*, 14885–14895; b) B. Bhartia, S. R. Puniredd, S. Jayaraman, C. Gandhimathi, M. Sharma, Y. C. Kuo, C. H. Chen, V. J. Reddy, C. Troadec, M. P. Srinivasan, *ACS Appl. Mater. Interfaces* **2016**, *8*, 24933–24945; c) H. Zheng, Y. Xu, J. Zhang, X. Xiong, J. Yan, L. Zheng, *J. Cleaner Prod.* **2017**, *143*, 269–277; d) C. Domingo, E. Loste, J. Fraile, *J. Supercrit. Fluids* **2006**, *37*, 72–86; e) S. Yan, B. Wang, Z. Wang, D. Hu, X. Xu, J. Wang, Y. Shi, *Biosens. Bioelectron.* **2016**, *80*, 34–38.
[18] a) Y. Ogomi, S. Sakaguchi, T. Kado, M. Kono, Y. Yamaguchi, S. Hayase, *J. Electrochem. Soc.* **2006**, *153*, A2294–A2297; b) Y. Tominaga, S. Tamagawa, *Ionics* **2016**, *23*, 337–342.
[19] S. Maniam, A. B. Holmes, J. Krstina, G. A. Leeke, G. E. Collis, *Green Chem.* **2011**, *13*, 3329–3332.
[20] C. Mindock, (Ed.: Reuters), Reuters, https://www.reuters.com/legal/litigation/forever-chemicals-were-everywhere-2023-expect-more-litigation-2024-2023-12-28/, **2023**.
[21] A. Willige, (Ed.: W. E. Forum), World Economic Forum, https://www.weforum.org/agenda/2024/03/pfas-forever-chemicals-eu-ban/, **2024**.
[22] A. Rensmo, E. K. Savvidou, I. T. Cousins, X. Hu, S. Schellenberger, J. P. Benskin, *Environ. Sci. Process. Impacts* **2023**, *25*, 1015–1030.
[23] a) Y. Zhao, O. Pohl, A. I. Bhatt, G. E. Collis, P. J. Mahon, T. Rüther, A. F. Hollenkamp, *Sustainable Chemistry* **2021**, *2*, 167–205; b) G. E. Collis, Q. Dai, J. S. C. Loh, A. Lipson, L. Gaines, Y. Zhao, J. Spangenberger, *Recycling* **2023**, *8*.
[24] a) M. Scully, B. Ledger, C. Johnson, (Ed.: Reuters), Reuters, https://www.reuters.com/legal/legalindustry/epa-developing-pfas-science-impacts-litigation-2024-01-30/, **2023**; b) X.-Z. Lim, *Nature* **2023**, *620*, 24–27.
[25] a) J. E. Rossini, A. S. Huss, J. N. Bohnsack, D. A. Blank, K. R. Mann, W. L. Gladfelter, *J. Phys. Chem. C* **2010**, *115*, 2–10; b) L. Zhang, J. M. Cole, *ACS Appl. Mater. Interfaces* **2015**, *7*, 3427–3455; c) J. W. Spalenka, P. Paoprasert, R. Franking, R. J. Hamers, P. Gopalan, P. G. Evans, *Appl. Phys. Lett.* **2011**, *98*; d) Y. S. Won, Y. S. Yang, J. H. Kim, J.-H. Ryu, K. K. Kim, S. S. Park, *Energy Fuels* **2010**, *24*, 3676–3681; e) J. Yu, T. L. Shen, W. H. Weng, Y. C. Huang, C. I. Huang, W. F. Su, S. P. Rwei, K. C. Ho, L. Wang, *Adv. Energy Mater.* **2011**, *2*, 245–252; f) C. J. Bruns, D. J. Herman, J. B. Minuzzo, J. A. Lehrman, S. I. Stupp, *Chem. Mater.* **2013**, *25*, 4330–4339; g) J. Jin, T. Iyoda, C. Cao, Y. Song, L. Jiang, T.-J. Li, D. B. Zhu, *Angew. Chem. Int. Ed.* **2001**, *40*; h) S. E. Brown-Xu, M. H. Chisholm, C. B. Durr, T. L. Gustafson, T. F. Spilker, *J. Am. Chem. Soc.* **2014**, *136*, 11428–11435.
[26] L. Lasser, E. Ronca, M. Pastore, F. De Angelis, J. Cornil, R. Lazzaroni, D. Beljonne, *J. Phys. Chem. C* **2015**, *119*, 9899–9909.
[27] M. A. M. Al-Alwani, A. B. Mohamad, N. A. Ludin, A. A. H. Kadhum, K. Sopian, *Renewable Sustainable Energy Rev.* **2016**, *65*, 183–213.
[28] a) Y. Shu, G. E. Collis, C. J. Dunn, P. Kemppinen, K. N. Winzenberg, R. M. Williamson, A. Bilic, T. B. Singh, M. Bown, C. R. McNeill, L. Thomsen, *J. Mater. Chem. C* **2013**, *1*; b) K. N. Winzenberg, P. Kemppinen, F. H. Scholes, G. E. Collis, Y. Shu, T. B. Singh, A. Bilic, C. M. Forsyth, S. E. Watkins, *Chem. Commun. (Camb.)* **2013**, *49*, 6307–6309; c) Y. Shu, A. Mikosch, K. N. Winzenberg, P. Kemppinen, C. D. Easton, A. Bilic, C. M. Forsyth, C. J. Dunn, T. B. Singh, G. E. Collis, *J. Mater. Chem. C* **2014**, *2*, 3895–3899; d) L. A. Stevens, K. P. Goetz, A. Fonari, Y. Shu, R. M. Williamson, J.-L. Brédas, V. Coropceanu, O. D. Jurchescu, G. E. Collis, *Chem. Mater.* **2015**, *27*, 112–118; e) P. A. White, G. E. Collis, M. Skidmore, M. Breedon, W. D. Ganther, K. Venkatesan, *New J. Chem.* **2020**, *44*, 7647–7658.
[29] T. W. Greene, P. G. M. Wuts, *Protective Groups in Organic Synthesis*, 3rd ed., John Wiley & Sons, Inc., **1999**.
[30] a) P. Gnida, M. Libera, A. Pająk, E. Schab-Balcerzak, *Energy Fuels* **2020**, *34*, 14344–14355; b) J. E. Rossini, A. S. Huss, J. N. Bohnsack, D. A. Blank, K. R. Mann, W. L. Gladfelter, *J. Phys. Chem. C* **2011**, *115*, 11–17; c) J. E. W. Beck, R. A. J. Janssen, *Adv. Funct. Mater.* **2002**, *12*, 519–525.
[31] S.-M. Chang, C.-L. Lin, Y.-J. Chen, H.-C. Wang, W.-C. Chang, L.-Y. Lin, *Org. Electron.* **2015**, *25*, 254–260.
[32] C. A. Garcia-Gonzalez, J. Saurina, J. S. Ayllon, C. Domingo, *J. Phys. Chem. C* **2009**, *113*, 13780–13786.
[33] a) R. Helmy, A. Y. Fadeev, *Langmuir* **2002**, *18*, 8924–8928; b) M. G. Gibby, A. Pines, J. S. Waugh, *JACS* **1972**, *94*; c) A. Franquet, M. Biesemans, R. Willem, H. Terryn, J. Vereecken, *J. Adhes. Sci. Technol.* **2004**, *18*, 765–778; d) T. Metroke, Y. Wang, W. J. van Ooij, D. W. Schaefer, *J. Sol-Gel Sci. Technol.* **2009**, *51*, 23–31; e) B. Xie, A. J. Muscat, *Microelectron. Eng.* **2005**, *82*, 434–440; f) A. J. Morris, G. J. Meyer, *J. Phys. Chem. C* **2008**, *112*, 18224–18231; g) W. J. Malfait, S. Zhao, R. Verel, S. Iswar, D. Rentsch, R. Fener, Y. Zhang, B. Milow, M. M. Koebel, *Chem. Mater.* **2015**, *27*, 6737–6745.
[34] G. A. Sewvandi, Z. Tao, T. Kusunose, Y. Tanaka, S. Nakanishi, Q. Feng, *ACS Appl. Mater. Interfaces* **2014**, *6*, 5818–5826.
[35] a) C. Dong, W. Xiang, F. Huang, D. Fu, W. Huang, U. Bach, Y. B. Cheng, X. Li, L. Spiccia, *Angew. Chem. Int. Ed. Engl.* **2014**, *53*, 6933–6937; b) S. Carli, L. Casarin, S. Caramori, R. Boaretto, E. Busatto, R. Argazzi, C. A. Bignozzi, *Polyhedron* **2014**, *82*, 173–180; c) J. Spivack, O. Siclovan, S. Gasaway, E. Williams, A. Yakimov, J. Gui, *Sol. Energy Mater. Sol. Cells* **2006**, *90*, 1296–1307; d) D. Song, H. An, J. H. Lee, J. Lee, H. Choi, I. S. Park, J. M. Kim, Y. S. Kang, *ACS Appl. Mater. Interfaces* **2014**, *6*, 12422–12428.

Manuscript received: March 14, 2024
Revised manuscript received: May 20, 2024
Accepted manuscript online: May 21, 2024
Version of record online: ■■, ■■

RESEARCH ARTICLE

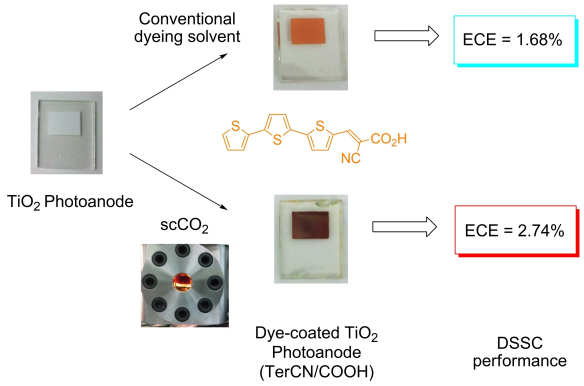

Go green: Silyl-masked oligothiophene dyes were successfully deposited onto TiO_2 photoanodes in using the green solvent, supercritical carbon dioxide in a short period of time and no waste solvent. Significant improvement in dye loading and solar cell device performance was achieved compared to devices fabricated using conventional organic solvent dye deposition methods. This approach could be applied to surface modification of substrates.

Dr. S. Maniam, Dr. M. Skidmore, Prof. Dr. G. A. Leeke, Dr. G. E. Collis**

Solar Cell Enhancement from Supercritical CO_2 Dye Surface Modification of Mesoporous TiO_2 Photoanodes